PHYSICAL REVIEW B **76**, 064432 (2007)

Low-energy spin dynamics in the giant keplerate molecule $\{Mo_{72}Fe_{30}\}$: A muon spin relaxation and ^1H NMR investigation

J. Lago,* E. Micotti, and M. Corti
Dipartimento di Fisica "A. Volta," University of Pavia and Unità CNR-INFM, I-27100 Pavia, Italy

A. Lascialfari†
Istituto di Fisiologia Generale e Chimica Biologica, University of Milano, I-20134 Milano, Italy;
CNR-INFM, I-27100 Pavia, Italy;
and S3-CNR-INFM, I-41100 Modena, Italy

A. Bianchi, S. Carretta, and P. Santini
Dipartimento di Fisica, Università di Parma, I-43100 Parma, Italy

D. Procissi,‡ S. H. Baek,§ and P. Kögerler
Ames Laboratory, Department of Physics and Astronomy, Iowa State University, Ames, Iowa 50011, USA

C. Baines and A. Amato
Paul Scherrer Institute, CH-5232 Villigen, Switzerland
(Received 4 April 2007; published 29 August 2007)

We present muon spin relaxation and ^1H NMR results on the magnetically frustrated keplerate molecule $\{Mo_{72}Fe_{30}\}$, aimed at studying the local spin dynamics as a function of temperature. We find that, in common with other molecular magnets, the relaxation spectrum of this material is characterized by a single dominating electronic correlation time τ. Experiments and theory show that τ has a thermally activated behavior with an activation gap of the order of the energy difference between the lowest-lying rotational bands in this material. This shows that, in the intermediate temperature range just above 1 K, the relaxation of the electronic spin system occurs via Orbach processes involving energy levels belonging to the two lowest-lying rotational bands. Our data thus provide an experimental estimate of the first interband gap.

DOI: 10.1103/PhysRevB.76.064432 PACS number(s): 75.45.+j, 76.60.−k, 76.75.+i

I. INTRODUCTION

A great deal of research has been devoted in the past few years to the preparation and study of novel so-called single molecule magnets, a group of solid materials constituted by a network of identical, iso-oriented magnetic molecules, each of them consisting of a relatively small cluster of ferro- or antiferromagnetically coupled magnetic ions embedded in an organic shell. With the clusters magnetically separated by these shells, macroscopic measurements yield to a large extent the amplified responses of the individual molecules and can be, therefore, directly related to them. This, together with the mesoscopic nature of the clusters, halfway between atomic and macroscopic scales, makes these materials ideal models for studying quantum size effects such as the quantum tunneling of the magnetization, the quantum coherence, etc.[1–3]

Ideally, one would also like to study the crossing from quantum to bulk cooperative behavior by increasing progressively the size of the magnetic cluster. This, however, eventually depends on the availability of molecular structures capable of accommodating increasing numbers of magnetic centers, something that might not be straightforward using traditional bridging ligands. Recently, however, new synthetic strategies[4,5] have led to the preparation of a new kind of highly symmetric polyoxomolybdate compound that opens up the possibility for such giant paramagnetic clusters. The compound $[Mo_{72}Fe_{30}O_{252}(Mo_2O_7(H_2O))_2(Mo_2O_8H_2(H_2O))(CH_3COO)_{12}(H_2O)_{91}]\cdot 150H_2O$, hereafter $Mo_{72}Fe_{30}$, is paradigmatic among these new *keplerates* and certainly one of the largest magnetic molecules prepared to date. The 30 Fe^{3+} ($s=5/2$) ions in this material occupy the vertices of an icosidodecahedron embedded in a framework of $\{(Mo)Mo_5\}$ groups that acts as an effective superexchange pathway despite the large nearest-neighbor Fe-Fe distance (6.4 Å),[6] leading to a relatively strong antiferromagnetic (AFM) coupling [$J=1.55$ K (Refs. 7 and 8)] and a ground state with net spin $S_T=0$. The system behaves as a simple paramagnet down to about 20 K, where the susceptibility departs from a simple Curie-Weiss law before reaching a plateau at 1 K. As a first approximation, the magnetism of $Mo_{72}Fe_{30}$ has been described by a classical Heisenberg model.[9,10] Since the icosidodecahedron (composed of 20 corner-sharing triangles) can be partitioned into three sublattices, the model leads to the same ground state spin arrangement as in the classical AFM triangle; that is, with nearest-neighbor spins at a relative angle of 120°. The model correctly predicts the quasilinear field dependence of the magnetization up to a critical field $B_c=17.7$ T, at which it saturates.[7]

As an alternative, a simplified quantum model based on a rotational band picture of the low-lying excitation spectrum has been proposed. This also accounts for the overall low-T behavior in this material. The concept of rotational bands

[i.e., $E \propto S(S+1)$, where E is the energy of each discrete level], which approximates the low-energy states of molecular ring structures with an even number of antiferromagnetically coupled Heisenberg spins,[11–14] also applies to other finite Heisenberg systems with AFM exchange, including nonbipartite, frustrated lattices such as the icosidodecahedron.[15] Thus, by considering an effective Hamiltonian which accounts for the three sublattices in $Mo_{72}Fe_{30}$, Schnack and co-workers derived an excitation spectrum whose lower part is formed by a set of parallel rotational bands, with the gap between the two lowest bands being 5 J (~8 K).[8,15,16] The presence of the first band has been further corroborated by a density-matrix renormalization study.[17] Experimentally, the observed temperature and field dependences of the magnetization are also consistent with the existence of the first quadratic band.[7,16] Evidence for higher order bands has been provided by a recent neutron scattering study, which shows a main mode centered at 0.6 meV (~8 K), interpreted as arising from transitions between the two lowest bands.[8] The details of the spectrum, especially its field dependence at base T, are not, however, entirely consistent with the model of Schnack and co-workers.

Here, we present a muon spin resonance (μSR) and NMR study of the local spin dynamics in $Mo_{72}Fe_{30}$ as a function of temperature ($0.02 < T < 300$ K) at various constant fields. Theoretical calculations of the nuclear spin-lattice relaxation rate $1/T_1$ are performed within the framework of the three-sublattice quadratic-band model. We find that $1/T_1$ probes the decay of the fluctuations of the total molecular magnetization produced by the magnetoelastic coupling with the phonon heat bath. At low T, this decay is mainly determined by a single type of relaxation process involving multistep Orbach paths passing through the first-excited rotational band. Therefore, these data provide further support for the three-sublattice quadratic-band model and highlight the possibility of obtaining the interband gap by studying the temperature behavior of the experimental NMR and μSR relaxation rates.

II. EXPERIMENTAL DETAILS AND RESULTS

A. Muon spin relaxation measurements

The polycrystalline samples of $Mo_{72}Fe_{30}$ under study were synthesized as reported in Ref. 5. Muon spin relaxation (μ^+SR) data were collected at various longitudinal field values in the temperature range $0.02 < T < 300$ K on the GPS and LTF beamlines at the LMU facility (PSI, Switzerland). For a review of the μ^+SR technique, see, for example, Ref. 18. Basically, information about the dynamics of the local fields in the sample is obtained by monitoring the positrons emitted by the muons during their decay in detectors placed in the forward (N_F) and backward (N_B) positions relative to the polarized muon beam. The muon-spin relaxation function (or asymmetry) is given by

$$G(t) = \frac{N_B(t) - \alpha N_F(t)}{N_B(t) + \alpha N_F(t)} = P_z(t) + a_{bk}, \qquad (1)$$

where a_{bk} is the contribution from muons stopped outside the sample and α is an instrumental parameter that accounts for the forward/backward detector efficiency. $P_z(t)$ describes the muon depolarization inside the specimen and thus provides information on the time evolution of the internal fields.

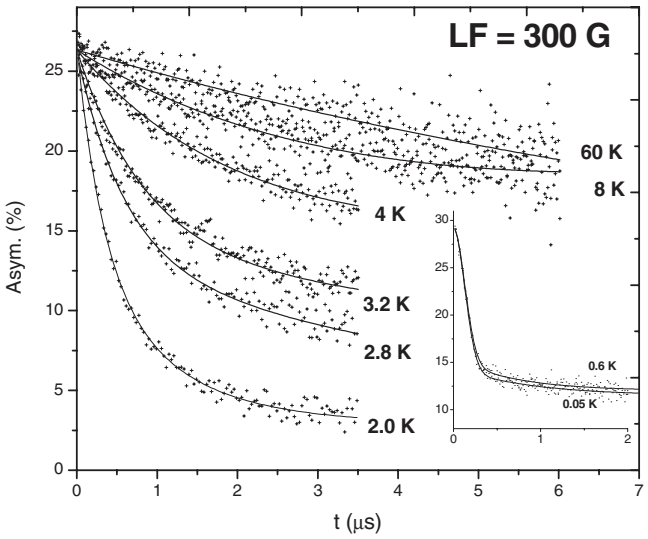

FIG. 1. Temperature dependence of the μ^+ polarization decay in LF=300 G. Solid lines represent the fits to Eq. (2) in the main text. Inset: ID for LTF ($T < 1$ K) data. Solid lines represent the fits to Eq. (3).

First, before presenting our μSR data and analysis, we want to point out that, in line with which has been previously observed for other molecular magnets (see, e.g., Refs. 11, 20, 21, and 32), we did not observe the formation of muonium in the present system as indicated by the constant initial asymmetry (close to the full value expected for the given geometry) throughout the entire temperature range.

Figure 1 shows the temperature evolution of the muon polarization for LF=300 G. Those at LF=2400 G are qualitatively identical. GPS data ($2 \leqslant T \leqslant 200$ K) were fitted to

$$G(t) = a_1 \exp(-\lambda_{1\mu SR} t) + a_2 \exp(-\lambda_{2\mu SR} t) + a_{bk}, \qquad (2)$$

where the total asymmetry and the relative weights of the two components were kept constant ($a_1/a_2 \approx 1.2$) over the entire T range. For LTF data ($T < 1$ K), on the other hand, the majority component shows a Gaussian relaxation, i.e.,

$$G(t) = a_1 \exp(-\sigma_1^2 t^2) + a_2 \exp(-\lambda_{2\mu SR} t) + a_{bk}. \qquad (3)$$

The temperature dependence of the various μ^+ relaxation rates obtained from fits to Eqs. (2) and (3) is shown in Fig. 2. The magnitude of the relaxation times is small and remains essentially unchanged on increasing LF, which *a priori* indicates that the relaxation is dynamical in nature; that is, we are probing spin-lattice relaxation processes associated with low-energy spin excitations. This, however, is in contrast with the Gaussian shape of the low-temperature (<1 K) curves, usually associated with depolarization caused by a distribution of static fields. We do not have, at the moment, a plausible explanation for this apparent contradiction, which, on the other hand, does not have a significant relevance in our analysis and discussion of the data.

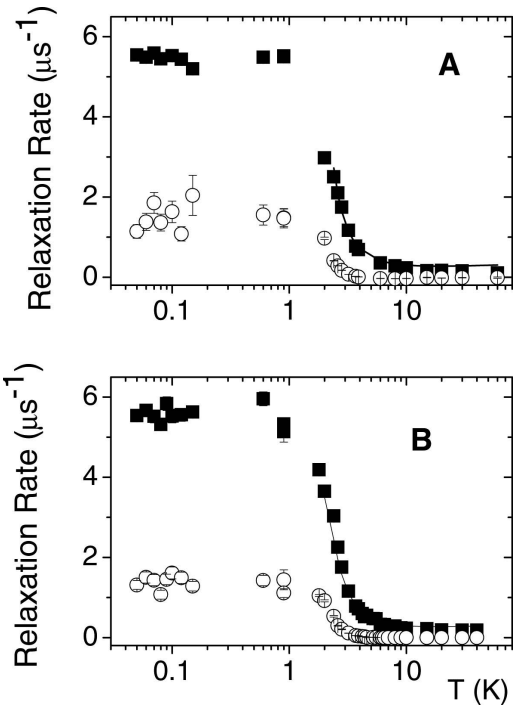

FIG. 2. Muon longitudinal relaxation rates $\lambda_{1\mu SR}$ ($\lambda_{1\mu SR} \equiv \sigma_1$ for $T < 1$ K) and $\lambda_{2\mu SR}$ corresponding to two different muon implantation sites (solid squares, $\lambda_{1\mu SR}$ or σ_1; empty circles, $\lambda_{2\mu SR}$) on $Mo_{72}Fe_{30}$ powders in LF=300 G (A) and 2400 G (B) obtained from the fit of the depolarization curves to Eq. (2) (GPS) and Eq. (3) (LTF) in the text. The solid lines represent the fit to Eq. (13) of the fastest rates, with the parameter values reported in the text. The Eq. (13) model fits also the slowest rates; fitting curves are not reported for clarity.

The observed two relaxation channels arise from the presence of at least two inequivalent muon stopping sites, the different magnitudes of the associated muon depolarization rates being, therefore, due to the difference in the total number of muons stopping in each inequivalent site. The magnitude of the different slow and fast relaxation rates $\lambda_{1\mu SR}(\sigma_1)$ and $\lambda_{2\mu SR}$ is due to different distances of muons from the Fe(III) magnetic ions, i.e., different intensity of the corresponding hyperfine interactions.

As already hinted by the raw curves, the relaxation remains slow and almost temperature independent down to ~4 K, where it shows a sharp increase before reaching a plateau for $T < 1$ K. Frequently, this can be associated with a thermally activated behavior of the electronic correlation time τ; in fact, the derived muon-relaxation rate $\lambda_{\mu SR}$ can be fitted above 1 K to a phenomenological exponential $\lambda_{\mu SR} = \lambda^0_{\mu SR} \exp(\Delta/T)$ with $\Delta \sim 10$ K. Note that in this T range, with the depolarization of the muon ensemble caused by dynamical fluctuations of the electronic spin system, one has $\lambda_{\mu SR} \propto B_i \tau/(1+\omega_L^2 \tau^2)$, where B_i is the rms average internal field, $\omega_L = \gamma_\mu B_{appl}$, and τ the characteristic time of the electronic fluctuations. Safely assuming $1/\tau \gg \omega_L$, it can be written that $\lambda_{\mu SR} \propto B_i \tau$; that is, the observed thermal behavior of the muon depolarization is simply reflecting the thermally activated behavior of the characteristic time τ, i.e., $\tau = \tau_0 \exp(\Delta/T)$, discussed below (see also NMR data on molecular rings[22] for a similar fitting model first used heuristically).

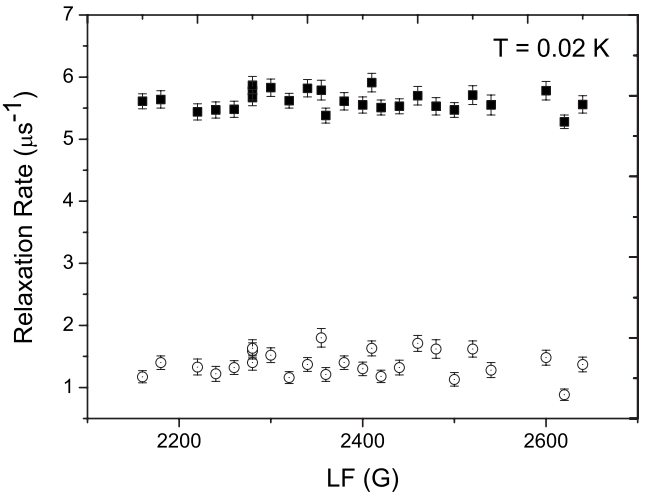

FIG. 3. Field dependence of the low-temperature longitudinal relaxation rates corresponding to the two muon implantation sites in $Mo_{72}Fe_{30}$ powders obtained from the fit to Eq. (3) of LTF data collected at $T=0.02$ K for LF values that span the calculated first level crossing ($B_0 \approx 2400$ G).

Finally, Fig. 3 shows the field dependence of the relaxation rates derived from the fit to Eq. (3) of data collected at $T=0.02$ K in LF values that span the calculated first level crossing in $Mo_{72}Fe_{30}$ [$B_0 \approx 0.24$ T (Ref. 16)]. Confirming preliminary results reported elsewhere,[20] there is no distinct feature in the relaxation of the system at the field B_0 that produces the crossing.

B. Nuclear magnetic resonance measurements

^1H NMR measurements were performed on $Mo_{72}Fe_{30}$ powders in the temperature range $1.5 \leqslant T \leqslant 300$ K at several magnetic field values using a standard Fourier-transform pulse spectrometer. The ^1H NMR spectrum consists of a single line with no peculiar structure, the width being due to the nuclear dipolar interaction.[11] The data referring to the temperature behavior of its full width at half maximum are reported in Ref. 19. The nuclear spin-lattice relaxation rate (NSLR, T_1^{-1}) was measured from the recovery of the nuclear magnetization obtained with a Hahn-echo sequence, following a series of saturating radio-frequency pulses. As already reported in previous work on this material,[19,20] this recovery deviates from a single exponential behavior due to the number of different inequivalent protons in the molecule, each with its own relaxation rate. The reported T_1^{-1}'s are, therefore, average values, estimated from the initial slope of the recovery curve following the common practice in these cases.[21] The thermal evolution of the relaxation rates for $B = 1.18$ and 2.75 T is presented in Fig. 4. Here, the solid lines represent the fits performed following the model presented in Sec. III. As for other molecular magnets,[19,22,23] $1/T_1(B,T)$ is characterized by a low-T maximum which shifts to higher T and reduces its intensity with increasing magnetic field.

III. THEORETICAL ANALYSIS AND DISCUSSION

In this section, we will first address the analysis of the temperature and field dependences of the NMR NSLR,

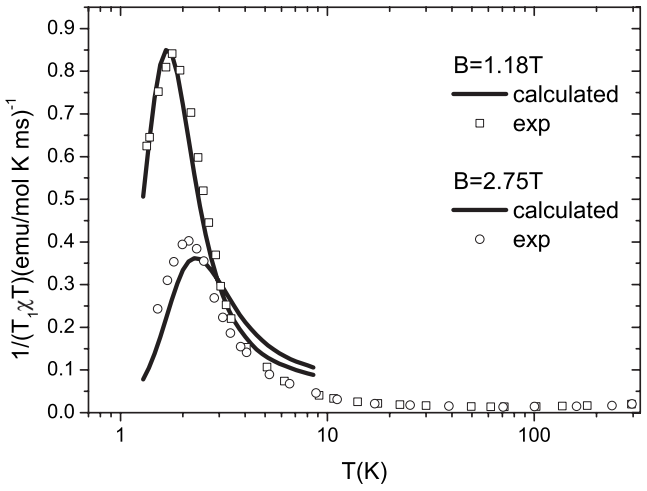

FIG. 4. $1/(T_1\chi T)$ vs T curves for two different values of the applied magnetic field B. The empty circles and squares are experimental data, while the solid and dashed lines are calculations (see text).

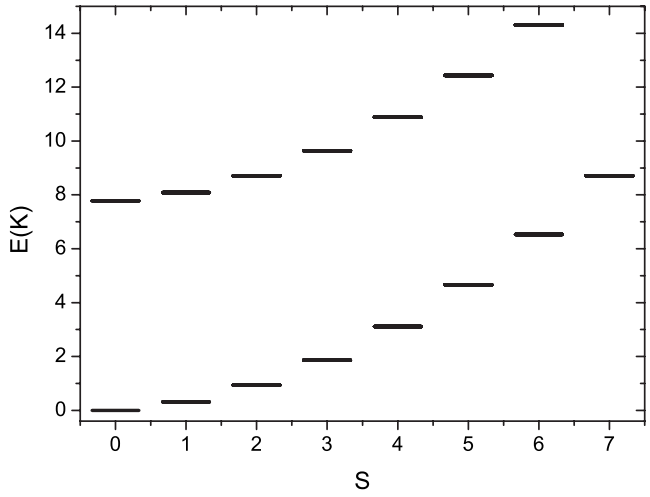

FIG. 5. The two lowest bands of energy levels calculated in zero field from the three-sublattice model (Refs. 8 and 16).

which will then be extended to the μ^+SR relaxation rate. Each Fe_{30} magnetic molecule can be described by the spin Hamiltonian

$$H = \sum_{i>j} J_{ij}\mathbf{s}_i \cdot \mathbf{s}_j + \sum_i \sum_{k,q} b_k^q(i) O_k^q(\mathbf{s}_i) + \sum_{i>j} \mathbf{s}_i \cdot \mathbf{D}_{ij} \cdot \mathbf{s}_j - g\mu_B \mathbf{B} \cdot \mathbf{S}, \quad (4)$$

where $\mathbf{s}_i$ are spin operators of the ith magnetic ion in the molecule. The first term is the isotropic Heisenberg exchange interaction. The second term describes the interactions with local crystal fields (CFs), with $O_k^q(\mathbf{s}_i)$ Stevens operator equivalents for the ith ion[24] and $b_k^q(i)$ CF parameters. The third term represents the dipolar anisotropic intracluster spin-spin interactions. The last term is the Zeeman coupling with an external field $\mathbf{B}$ [$g=1.974$ (Ref. 9)], with $\mathbf{S}$ the total spin. The dimension of the Hilbert space for Fe_{30} is huge [6^{30}] and precludes the numerical diagonalization of H on any computer. Recently, an approximate three-sublattice model has been proposed and exploited to analyze inelastic neutron scattering results.[8,16] By naming $\mathbf{S}_A$, $\mathbf{S}_B$, and $\mathbf{S}_C$ the total spin of the three sublattices, the low-energy spin dynamics of Fe_{30} is approximately described by

$$H_{eff} = J(\mathbf{S}_A \cdot \mathbf{S}_B + \mathbf{S}_A \cdot \mathbf{S}_C + \mathbf{S}_B \cdot \mathbf{S}_C)/5 - g\mu_B \mathbf{B} \cdot \mathbf{S}, \quad (5)$$

where $J=1.55$ K is the nearest-neighbor exchange constant and $\mathbf{S}$ is the total spin of the molecule. Eigenvalues of H_{eff} can be analytically calculated as

$$E(S_A,S_B,S_C,S,M) = J[S(S+1) - S_A(S_A+1) - S_B(S_B+1) - S_C(S_C+1)]/10 - g\mu_B BM, \quad (6)$$

with M the eigenvalue of the z component of the total spin. The system has a nonmagnetic $S=0$ ground state, whereas the low-lying excited states form a set of parabolic "rotational" bands (see Fig. 5). The lowest band is composed of 132 651 levels, while the second rotational band contains 3 441 123 states.

Since Fe^{3+} ions are arranged on the vertices of an icosidodecahedron, Fe_{30} offers the possibility of studying the relaxation behavior of a highly frustrated system. The low-frequency quasielastic (QE) spin dynamics is calculated as in Ref. 29. The interaction with the phonon heat bath leads to the following expression for the Fourier transform of the time autocorrelation function for equilibrium fluctuations of two generic observables $\mathcal{A}$ and $\mathcal{B}$:

$$S_{\mathcal{A},\mathcal{B}}(\omega) = \sum_{q,t} (\mathcal{B}_{tt} - \langle\mathcal{B}\rangle_{eq})(\mathcal{A}_{qq} - \langle\mathcal{A}\rangle_{eq}) \mathrm{Re}\left(p_t^{eq}\left(\frac{1}{i\omega - \mathbf{W}}\right)_{qt}\right), \quad (7)$$

where $p_t^{(eq)}$ is the equilibrium population of the tth level, $\mathcal{B}_{tt}=\langle t|\mathcal{B}|t\rangle$, and $\mathbf{W}$ is the so-called rate matrix. Its elements W_{st} represent the probability per unit time that a transition between levels $|t\rangle$ and $|s\rangle$ is induced by the interaction with the heat bath. The QE frequency spectrum is therefore a sum of n Lorentzians centered at zero frequency whose widths λ_i are the eigenvalues of $-\mathbf{W}$ (n being the dimension of the molecule spin Hilbert space). As noted in Ref. 29, these n λ_i are different from the n inverse level lifetimes.

The main contribution to the spin-phonon coupling potential V comes from the modulation of isotropic exchange and of rank-2 intramolecular anisotropic interactions by elastic waves. However, experimental information is by far insufficient to assess the specific form of V. Moreover, even if V was known, it would not be sensible to calculate the W_{st} matrix elements. Their calculation requires knowledge of the complex composition of each eigenstate in terms of local spin states, and this is not set by the three-sublattice model. In view of this, the most unbiased choice is to assume $v=|\langle t|V|s\rangle|^2=1$ if the selection rules $|\Delta S|=0,1,2$; $|\Delta S_A|=0,1,2$; $|\Delta S_B|=0,1,2$; $|\Delta S_C|=0,1,2$; $|\Delta S_{AB}|=0,1,2$; and $|\Delta M|=0,1,2$ are satisfied, and $v=0$ otherwise ($\mathbf{S}_{AB}=\mathbf{S}_A+\mathbf{S}_B$). This sort of approximation is analogous to that used in Ref. 8 for the interpretation of neutron spectroscopy data. By

adopting a Debye model for phonons, for allowed transitions, this leads to

$$W_{st} = \gamma \pi v \Delta_{st}^3 n(\Delta_{st}), \tag{8}$$

with

$$n(x) = (e^{\beta \hbar x} - 1)^{-1}, \quad \Delta_{st} = (E_s - E_t)/\hbar.$$

The free parameter γ describes the spin-phonon coupling strength, and is determined by comparison with experimental data. Even within this approximation, calculating the relaxation spectrum [Eq. (7)] by including all the states belonging to the two lowest bands is unfeasible because of the huge dimension of the resulting Hilbert space (3 573 774 states). Therefore, in order to calculate the relaxation dynamics of Fe_{30}, we have made two further approximations. First, we have limited our calculations to low temperature, thus including levels with energy only up to 11.1 K (9.3 K) from the (field dependent) ground state for $B=1.18$ T ($B=2.75$ T), and higher-lying levels of the two lowest bands connected to these by V. For each of these eigenstates of the second band, there are eight further degenerate eigenstates having the same set of quantum numbers $(S_A, S_B, S_C, S_{AB}, S, M)$. To further reduce the dimension of the spin Hilbert space, we have considered only one representative state (out of nine), and we have multiplied interband transition probabilities by 9. We have checked that if both these approximations are relaxed, results do not change qualitatively.

Important information on the relaxation dynamics of Fe_{30} can be obtained through NMR measurements of the nuclear spin-lattice relaxation rate $1/T_1$.[29] The latter is given by a linear combination of the Fourier transforms of electronic spin correlation functions evaluated at the Larmor frequency.[25,27,28,30] By considering only the Heisenberg and Zeeman terms in H [Eq. (4)], the spin-lattice relaxation rate of a magnetic nucleus of Larmor frequency ω_L interacting with a molecule composed of N spins may be written as

$$\frac{1}{T_1} \propto \sum_{i,j=1,N} \alpha_{ij}[S_{s_i^z,s_j^z}(\omega_L) + S_{s_i^z,s_j^z}(-\omega_L)] + \beta_{ij}[S_{s_i^+,s_j^-}(\omega_L) + S_{s_i^+,s_j^-}(-\omega_L) + S_{s_i^-,s_j^+}(\omega_L) + S_{s_i^-,s_j^+}(-\omega_L)], \tag{9}$$

where α_{ij} and β_{ij} are geometrical coefficients of the dipolar interaction between nuclear and electronic spins, and $S_{A,B}(\omega)$ is the Fourier transform of the time correlation function. Since far from level crossings $\omega_L \ll \Delta_{st}$, only the QE part of the $S_{A,B}(\omega)$ in the above formula contributes to $1/T_1$.[26] If magnetic anisotropy is neglected, Eq. (7) implies that only zz terms are nonzero in Eq. (9) because $\langle s|s_i^{\pm}|s\rangle = \langle t|s_i^{\pm}|t\rangle = 0$. In addition, within the three-sublattice model, $\langle s|s_{i,z}|s\rangle \propto \langle s|S_z|s\rangle$. Therefore, within the present model, the nuclear spin-lattice relaxation rate is proportional to the Fourier transform of the autocorrelation function of S_z:

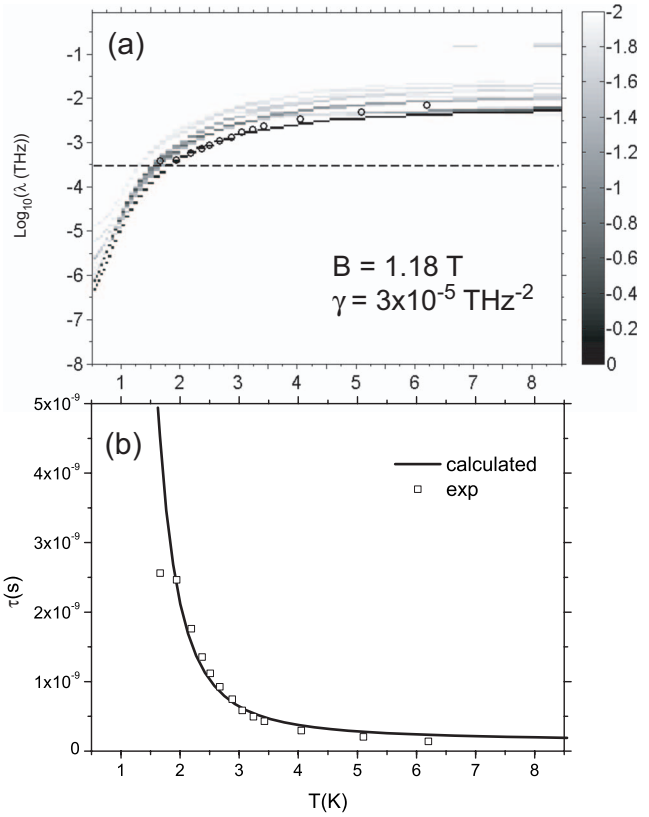

FIG. 6. (a) Calculated frequency spectra $A(\lambda_i, T, B)$ of the magnetization autocorrelation $S_{S_z,S_z}(\omega)$ as a function of T. The gray scale maps $\log_{10}[A/\chi T]$ and gives the weight of each Lorentzian in the spectrum of fluctuation of S_z. For each value of T, the ω-integrated weight equals the size of equilibrium fluctuations, proportional to χT. The dashed line represents the ^1H Larmor angular frequency ω_L, and the white points are the characteristic frequency $\lambda_0(T)$ extracted from experimental NMR data [see Fig. 6(b)]. The graphic shows only the frequency weights larger than 1%. (b) Calculated (line) and measured (squares) relaxation time τ_0^{mag} for $B=1.18$ T. The line corresponds to the dominant frequency λ_0 in Fig. 6(a). The T dependence of τ_0^{mag} follows an Arrhenius law with a gap $\Delta \approx 7.2$ K.

$$1/T_1 \propto S_{S_z,S_z}(\omega_L). \tag{10}$$

Hence, in Fe_{30} a measure of $1/T_1$ allows one to directly extract information on the decay of the autocorrelation of the molecular magnetization. Therefore, in the following, we focus on the case $\mathcal{A}=\mathcal{B}=S_z$; i.e., we study the spectrum of fluctuations of the molecular magnetization. In general, many different relaxation frequencies $\lambda_i(T,B)$ can contribute to this spectrum:

$$S_{S_z,S_z}(\omega,T,B) = \sum_{i=1,n} A(\lambda_i,T,B)\frac{\lambda_i(T,B)}{\lambda_i(T,B)^2 + \omega^2}. \tag{11}$$

Figure 6(a) shows logarithmic intensity plots of the frequency weights $A(\lambda_i, T, B)$ as function of temperature T. The free parameter $\gamma = 3 \times 10^{-5}$ THz^{-2} has been estimated by fitting the position of the peaks observed in the T dependence of $1/T_1$ (see below). The precise value of γ does not change

the spectra qualitatively, but merely sets the frequency scale. Surprisingly, *a single Lorentzian* of characteristic frequency λ_0 dominates the relaxation spectrum of S_z for a fairly wide range of values of T and B. By exploiting linear response theory, the dynamical structure can be approximately rewritten as

$$S_{S_z,S_z}(\omega,T,B) \propto \chi T \frac{\lambda_0(T,B)}{\lambda_0(T,B)^2+\omega^2}, \tag{12}$$

where χT is the magnetic susceptibility times the temperature, and represents a quantity proportional to the effective magnetic moment μ_{eff}. The single dominating decay time $\tau_{QE}=\lambda_0^{-1}$ is different from the lifetime of any thermally populated level. Our calculations indicate that in the single Lorentzian regime, the decay of fluctuations of the molecular magnetization is mostly due to interband Orbach-like processes. In particular, the dominant relaxation time τ_{QE} follows, at low T, an Arrhenius law $\tau \propto \exp(\Delta/T)$ with $\Delta \approx 7.2$ K (for $B=1.18$ T) [Fig. 6(b)], which is close to the energy gap between the two lowest energy bands. Direct intraband transitions do not appreciably affect the relaxation behavior due to the small associated gaps.

Since there is only a single frequency with appreciable weight in the spectrum of fluctuations, Eq. (10) implies (see Fig. 4) that $1/(T_1\chi T)$ displays a sharp peak at the temperature T_0 for which $\lambda_0(T_0)=\omega_L$, i.e., where the horizontal dashed line intersects the black curve in Fig. 6(a). In spite of the unavoidable approximations made in the calculation, the agreement between theoretical and experimental results in Figs. 6 and 4 is very good and provides strong support to our picture of relaxation dynamics in Fe_{30}. In particular, a single thermally activated Orbach process sets the decay of S_z, just as found in AF rings, AF grids, and high-anisotropy nanomagnets.[29,31] This in spite of the very different spectrum of the highly frustrated Fe_{30} molecule.

In contrast to the NSLR, the muon-relaxation rate obtained from the analysis above (see Fig. 2) does not peak at low T. In fact, it flattens for $T \leqslant 1$ K to a common value $\lambda_0 \sim 5.5\ \mu s^{-1}$ for the two applied fields used in the experiment. This cannot be the result of the different hyperfine coupling of μ^+ and ^1H since, if we are probing spin dynamics at the Larmor frequency ω_L, the relaxation rates of the two species should just differ by a scaling factor and their T dependence should be the same. It seems therefore that, in this temperature range, the μ^+SR rate is probing relaxation processes other than those probed by NMR. The reason for this behavior is not well understood, and here below, we limit ourselves to introducing different possible hypotheses.

First, we notice that the presence of low-T spin fluctuations whose frequencies do not depend on temperature is commonly ascribed to the relaxation of the electronic spin system via a quantum mechanical mechanism and has been found ubiquitous among geometrically frustrated systems due to the large ground state degeneracy. Since the Fe^{3+} ions in $Mo_{72}Fe_{30}$ sit on the vertex of a frustrated, albeit finite, lattice (thus leading to a relatively high degeneracy of the energy levels[16]), a similar explanation could, in principle, be valid for this material.

Alternatively, the μ^+SR signal may not be picking up the intrinsic dynamics of the electronic spin system, which could be the case if the depolarization of the muon ensemble is no longer dominated by electronic spin dynamics, once the Orbach process that dominates above ~ 1 K becomes irrelevant at lower T, but by the quasistatic T-independent dipolar interactions of intermolecular origin (note that the LTF curves in Fig. 1 show a Gaussian front end, usually associated with a distribution of static internal fields). However, a detailed calculation of, first, the muon stopping site(s) and then of the dipolar fields sensed at this position must be carried out before a definitive answer to this question is produced.

Finally, we would like to remark that the observed behavior is unlikely to be the result of an improper thermalization (measurements were made on powder samples) as T-independent muon relaxation has been previously observed in other molecular magnets at temperatures as high as ~ 40 K in V15,[32] well above the region where thermalization of the sample could be a problem.

Whatever the muon-relaxation mechanism below 1 K, the rise in the muon-relaxation rate occurring at higher T can be analyzed in the same way as the NSLR. Following the same arguments as in NMR, one arrives at an expression for the muon depolarization rate formally identical to Eq. (12). In fact, following Ref. 32 (and in analogy to the paper regarding NMR data, i.e., Ref. 22), it can be written

$$\lambda_{\mu SR}(T,B) = A\chi T \frac{\lambda_0(T,B)}{\lambda_0(T,B)^2+\omega_L^2}, \tag{13}$$

where λ_0 has its current meaning, A is the average of the hyperfine field fluctuations at the muon site(s), and ω_L is the Larmor frequency of the muon. By assuming $\lambda_0 = (1/\tau_0)\exp(-\Delta/T)$, the fitting procedure regarding the fastest relaxation rates (the same fitting model is valid for the slowest component; data are not reported for the sake of clarity) for $B=300$ and 2400 G in the temperature interval $1.5 < T \leqslant 10$ K gives $A = 1.09 \times 10^{16}$ rad^2/s^2, $\tau_0 = 0.2 \times 10^{-10}$ s, and $\Delta = 10.5(5)$ K. These results confirm the presence of a single dominating electronic correlation time with activated behavior. We can finally note that, apart from the effects on A due to different hyperfine coupling constants and gyromagnetic ratios, the position of the muons (interstitial) and protons (at crystal sites) does not influence the revealed results about spin dynamics. This is the expected consequence of a difference in geometrical location of a local probe with respect to the magnetic [Fe(III)] center.

IV. CONCLUSIONS

We have presented a NMR and μ^+SR study of the temperature dependence of electronic spin dynamics in $Mo_{72}Fe_{30}$. We find that in the intermediate temperature regime (above ~ 1 K), both the NMR and μ^+SR longitudinal relaxation rates show a unique dominating correlation time characterized by a thermally activated behavior with an activation energy roughly equivalent to the gap between the lowest rotational bands of this material. These results are consistent with our theoretical calculations, which show that

a single interband Orbach process dominates the low-E excitation spectrum in this regime.

As for other molecular magnets, the μ^+SR relaxation rate becomes independent of T for temperatures below the maximum in NSLR. The physical mechanism responsible for this flattening, possibly of quantum origin, is still under investigation.

ACKNOWLEDGMENTS

The authors want to thank P. Carretta and G. Amoretti for useful discussions and suggestions. This work was supported by FIRB RBNE01YLKN-2001, RTN HPRN-CT-00012 Quemolna, and NoE MAGMANET.

*lago@fisicavolta.unipv.it
†lascialfari@fisicavolta.unipv.it
‡Present address: Brain Imaging Center, CalTech, Pasadena, CA 91125.
§Present address: NHMFL FSU, Tallahassee, FL 32310-3706.

[1] L. Thomas, F. Lionti, R. Ballou, D. Gatteschi, R. Sessoli, and B. Barbara, Nature (London) **383**, 145 (1996).
[2] R. Sessoli, D. Gatteschi, A. Caneschi, and M. A. Novak, Nature (London) **365**, 141 (1993).
[3] W. Wernsdorfer and R. Sessoli, Science **284**, 133 (1999).
[4] A. Müller, E. Krickmeyer, H. Bögge, M. Schmidtmann, and F. Peters, Angew. Chem., Int. Ed. **37**, 3360 (1998).
[5] A. Müller, S. Sarkar, S. Q. Nazir Shah, H. Bögge, M. Schmidtmann, S. Sarkar, P. Kögerler, B. Hauptfleisch, A. X. Trautwein, and V. Schünemann, Angew. Chem., Int. Ed. **38**, 3238 (1999).
[6] A. Müller, P. Kögerler, and A. W. M. Dress, Coord. Chem. Rev. **222**, 193 (2001).
[7] A. Müller, M. Luban, C. Schröder, R. Modler, P. Kögerler, M. Axenovich, J. Schnack, P. Canfield, S. Bud'ko, and N. Harrison, ChemPhysChem **2**, 517 (2001).
[8] V. O. Garlea, S. E. Nagler, J. L. Zarestky, C. Stassis, D. Vaknin, P. Kögerler, D. F. McMorrow, C. Niedermayer, D. A. Tennant, B. Lake, Y. Qiu, M. Exler, J. Schnack, and M. Luban, Phys. Rev. B **73**, 024414 (2006).
[9] M. Axenovich and M. Luban, Phys. Rev. B **63**, 100407(R) (2001).
[10] M. Hasegawa and H. Shiba, J. Phys. Soc. Jpn. **73**, 2543 (2004).
[11] A. Lascialfari, D. Gatteschi, F. Borsa, and A. Cornia, Phys. Rev. B **55**, 14341 (1997).
[12] M.-H. Julien, Z. H. Jang, A. Lascialfari, F. Borsa, M. Horvatić, A. Caneschi, and D. Gatteschi, Phys. Rev. Lett. **83**, 227 (1999).
[13] G. L. Abbati, A. Caneschi, A. Cornia, A. Fabretti, and D. Gatteschi, Inorg. Chim. Acta **297**, 291 (2000).
[14] S. Carretta, J. van Slageren, T. Guidi, E. Liviotti, C. Mondelli, D. Rovai, A. Cornia, A. L. Dearden, F. Carsughi, M. Affronte, C. D. Frost, R. E. P. Winpenny, D. Gatteschi, G. Amoretti, and R. Caciuffo, Phys. Rev. B **67**, 094405 (2003).
[15] J. Schnack and M. Luban, Phys. Rev. B **63**, 014418 (2000).
[16] J. Schnack, M. Luban, and R. Modler, Europhys. Lett. **56**, 863 (2001).
[17] M. Exler and J. Schnack, Phys. Rev. B **67**, 094440 (2003).
[18] P. Dalmas de Reotier and A. Yaouanc, J. Phys.: Condens. Matter **9**, 9113 (1997).
[19] J. K. Jung, D. Procissi, R. Vincent, B. J. Suh, F. Borsa, P. Kögerler, C. Schröder, and M. Luban, J. Appl. Phys. **91**, 7388 (2002).
[20] E. Micotti, D. Procissi, A. Lascialfari, P. Carretta, P. Kögerler, F. Borsa, M. Luban, and C. Baines, J. Magn. Magn. Mater. **272-276**, 1099 (2004).
[21] F. Borsa, A. Lascialfari, and Y. Furukawa, in *Novel NMR and EPR Techniques*, edited by J. Dolinsek, M. Vilfan, and S. Zumer (Springer, Berlin, 2006), pp. 297–349.
[22] S. H. Baek, M. Luban, A. Lascialfari, E. Micotti, Y. Furukawa, F. Borsa, J. van Slageren, and A. Cornia, Phys. Rev. B **70**, 134434 (2004).
[23] D. Procissi, B. J. Suh, E. Micotti, A. Lascialfari, Y. Furukawa, and F. Borsa, J. Magn. Magn. Mater. **272-276**, 741(E) (2004).
[24] A. Abragam and B. Bleany, *Electron Paramagnetic Resonance of Transition Ions* (Clarendon, Oxford, 1970).
[25] T. Moriya, Prog. Theor. Phys. **16**, 23 (1956); **28**, 371 (1962).
[26] Direct incoherent transitions between degenerate levels have been neglected due to the vanishing phonon density of states.
[27] D. Hone, C. Scherer, and F. Borsa, Phys. Rev. B **9**, 965 (1974).
[28] F. Borsa and A. Rigamonti, *Magnetic Resonance of Phase Transitions* (Academic, New York, 1979).
[29] P. Santini, S. Carretta, E. Liviotti, G. Amoretti, P. Carretta, M. Filibian, A. Lascialfari, and E. Micotti, Phys. Rev. Lett. **94**, 077203 (2005).
[30] C. P. Slichter, *Principles of Magnetic Resonance* (Springer-Verlag, Berlin, 1992).
[31] M. Corti, M. Filibian, P. Carretta, L. Zhao, and L. K. Thompson, Phys. Rev. B **72**, 064402 (2005).
[32] D. Procissi, A. Lascialfari, E. Micotti, M. Bertassi, P. Carretta, Y. Furukawa, and P. Kögerler, Phys. Rev. B **73**, 184417 (2006).